

High-precision Elevation Sensor Based on Atmospheric Pressure

Gou Jie,¹ Zhu Hao,^{2,3} and Yang Huadong^{2,3*}

¹Wuhan Technical College of Communication, Wuhan 430065, China

²CCCC Second Harbor Engineering Company Ltd., No. 11 Jinyinhu Road, Dongxihu District, Wuhan, China

³Key Laboratory of Transportation Sector for Long-Span Bridge Construction Technique, Wuhan 430040, China

(Received July 14, 2023; accepted November 30, 2023)

Keywords: dynamic differential, barometric altimeter, moving average

The traditional method of calculating the height of a measurement point through atmospheric pressure and standard atmospheric models ignores the irregular changes in the atmosphere, resulting in significant errors. In this paper, a mathematical model for dynamic differential measurement is derived on the basis of the basic atmospheric pressure-height theoretical model. Then, a high-precision elevation sensor based on atmospheric pressure is developed using IoT technology, and a real-time dynamic differential measurement system is established. By establishing a ground reference station to dynamically calibrate the errors caused by atmospheric changes in real time, high-precision and highly reliable real-time elevations are obtained through calculation. The experiment shows that the average measurement error due to dynamic differences is less than 5 cm. At the same time, we also use the sliding average filtering method to effectively improve the real-time measurement accuracy while ensuring the constant measurement frequency. The measurement error is reduced from ± 15 to ± 5 cm, and the measurement results can be uploaded to a cloud platform in real time, with good engineering practicality.

1. Introduction

Elevation is an important information for the three-dimensional positioning of personnel, vehicles, components, and so forth, and its measurement accuracy directly affects the reliability and accuracy of positioning. At present, the elevation measurement mainly uses the global navigation satellite system (GNSS), in which the GNSS-Interferometric/Multipath R technology uses the signal-to-noise ratio, pseudo-range, and oscillation phenomenon of carrier phase timing sequence output by the navigation receiver to measure the surface parameters.^(1–4) For example, Roggenbuck *et al.* used this method to measure the sea surface significant wave height.⁽⁵⁾ Strandberg *et al.* combined the unscented Kalman filter and B-spline interpolation to measure the height of the sea surface with an accuracy higher than 5 cm.⁽⁶⁾ However, when in tunnels, bridges, mountainous areas, and high-rise buildings or when GNSS is closed, the lack of satellite signals received by GNSS will lead to a decrease in positioning accuracy or even a failure in positioning.^(7–9) The air pressure sensor is not affected by satellite occlusion and human factors.

*Corresponding author: e-mail: 464179071@qq.com

<https://doi.org/10.18494/SAM4575>

It can obtain elevation information indirectly by sensing atmospheric pressure and according to the single value function relationship between air pressure and altitude. Therefore, with further improvement of the barometric sensor, it can be applied to the supplementation and improvement of the GNSS elevation positioning. Ai and coworkers introduced the concept and method of barometric height measurement as a virtual constellation to the China regional positioning system based on a communication satellite to supplement and improve the feasibility of three-dimensional positioning.^(10,11) Xia *et al.* used multiple barometers as reference nodes to match the pedestrian's air pressure signal with the reference node's air pressure to locate the pedestrian's height.⁽¹²⁾ Choo *et al.* estimated the altitudes of workers on the basis of the atmospheric pressure measured by a barometer and acceleration and gyroscopic signals from an inertial measurement unit, which can be used in the safety identification of on-site construction personnel.⁽¹³⁾ However, if irregular changes in the atmosphere are ignored, there will be large errors when calculating the height through the atmospheric pressure and the standard atmospheric model. Therefore, in this paper, we propose a high-precision elevation sensor based on atmospheric pressure and dynamic difference, optimize the mathematical model of height measurement based on atmospheric pressure, and use the moving average method to process the measurement results numerically, realizing the high-precision measurement of height.

2. Principle of Dynamic Differential Measurement

The method of using a barometer for elevation measurement has a long history, and through continuous development, its technical theory has become relatively mature. In the atmosphere, there is an inherent relationship between atmospheric pressure and altitude, that is, within a certain altitude range, the atmospheric pressure continuously decreases as the altitude increases. On the basis of this relationship, when the atmospheric pressure at a certain altitude is measured, the altitude at that point can be calculated according to the corresponding functional relationship. To obtain an ideal height measurement model in an actual height measurement, it is often necessary to make some assumptions. There are two common models: an isothermal atmospheric hypothesis model and an international standard atmospheric pressure height model.

In the isothermal atmospheric hypothesis model, it is assumed that the temperature of the measurement location area does not change in the height direction, and both are T , according to the ideal state gas equation:⁽¹⁴⁾

$$P = R_d \rho T, \quad (1)$$

where P represents the atmospheric pressure intensity, R_d is the universal pressure constant, ρ is the density of the ideal gas, and T is the Kelvin temperature of the current environment, set to a constant value. According to the theory of atmospheric statistics, the relationship between atmospheric pressure and altitude can be expressed as

$$dP = -g \rho dh, \quad (2)$$

where g is the average sea level acceleration. From Eqs. (1) and (2),

$$\frac{dP}{P} = -\frac{g}{R_d T} dh, \quad (3)$$

can be obtained.

The International Organization for Standardization has made uniform regulations on some important atmospheric parameters, as shown in Table 1.⁽¹⁵⁾

It is necessary to measure the atmospheric pressure P_0 at the ground level in the positioning area, assume that the height at the ground level is 0, and record the indoor ambient temperature t (°C) when measuring the atmospheric pressure data. According to the isothermal atmospheric hypothesis model, when the atmospheric pressure measured by the barometer at the height of the mobile node is P , the height of the mobile node relative to the ground is

$$h = 18410 \left(1 + \frac{t}{273.15}\right) \lg \frac{P_0}{P}. \quad (4)$$

However, because the impact of temperature fluctuations on atmospheric pressure measurement is ignored, this model is only suitable for scenarios where indoor temperature is relatively stable. In practical application scenarios, considering the impact of temperature fluctuations, the international standard atmospheric pressure height formula can be selected for elevation measurement. For the temperature gradient of air pressure β , we have the following relationship between isobaric layer temperature and height:^(16,17)

$$T = T_0 - \beta(h - h_0). \quad (5)$$

Therefore,

$$dT = -\beta dh. \quad (6)$$

We substitute Eq. (6) into Eq. (3) and integrate both sides simultaneously to obtain

$$\ln \frac{P}{P_0} = \frac{g}{R_d \beta} \ln \frac{T}{T_0}. \quad (7)$$

Table 1
Main parameters of international standard atmosphere.

Parameter	Nominal value
Mean sea level acceleration	$g = 9.80665 \text{ m/s}^2$
Mean sea surface temperature	$T_0 = 288.15 \text{ K}$
Temperature gradient	$B = -6.5 \times 10^{-3} \text{ K/m}$
Universal barometric parameters	$R_d = 287.05287 \text{ m}^2/(\text{s}^2\text{K})$

From Eqs. (5) and (7), we can obtain

$$h - h_0 = \frac{T_0}{\beta} \left[1 - \left(\frac{P}{P_0} \right)^{\frac{\beta R_d}{g}} \right]. \quad (8)$$

If the values of the parameters in Table 1 are substituted and the sea level height is zero, the absolute height relative to sea level can be expressed as

$$h = 44330.77 \left[1 - \left(\frac{P}{101325} \right)^{0.1902631} \right]. \quad (9)$$

The basic idea of differential measurement is to set a reference point on the ground in the measurement area to dynamically calibrate the elevation measurement error caused by air pressure and temperature changes. During the measurement, the actual elevation of the reference point should remain unchanged, but owing to the instability of air pressure and temperature, the measured height of the reference point changes moment by moment. Since the datum and measuring points are located in the same area, air pressure and temperature fluctuations can be approximately equal, so the measurement error can be compensated in real time by measuring the fluctuation of the datum point.

Assuming that the virtual reference point remains unchanged, the measured height fluctuation of the reference point is expressed as

$$\Delta h = h_0' - h_0. \quad (10)$$

The height of the measuring point after real-time compensation calibration can be expressed as

$$h = h' - \Delta h = h_0 + h' - h_0', \quad (11)$$

where h_0 represents the calibrated reference point height, h' represents the measured height of the measurement sensor, and h_0' represents the measured height of the base station sensor.

For the isothermal atmospheric pressure high model, considering the existing temperature differences in the height direction, we conducted some optimization processing, taking the average of two measurement points as a constant stable value.

$$t_m = \frac{t + t_0}{2} \quad (12)$$

By substituting Eq. (12) into Eq. (4) and the result into Eq. (11), the elevation calculation formula for differential measurement under the isothermal atmospheric pressure high model can be obtained as

$$h = h_0 + 18410 \left(1 + \frac{t + t_0}{256.3} \right) \lg \frac{P_0}{P}. \quad (13)$$

3. Sensor Design

To realize the dynamic differential measurement, two conditions should be met: (1) data synchronization between the reference sensor and the measurement sensor and (2) the real-time processing of the data. The basic design idea is that a reference sensor sends a measurement command and each measurement sensor responds by returning the measured pressure and temperature. The reference sensor performs differential processing on the returned data to calculate the height and then sends it to the cloud platform or designated server through a wireless transmission module. The specific dynamic differential measurement process and data interaction method are as follows:

- Step 1: Set the response timing and response delay of each measurement sensor in the software.
- Step 2: The reference sensor sends a start measurement command Start to each measurement sensor.
- Step 3: After receiving the Start command, the measurement sensor sequentially collects air pressure and temperature data according to the response timing and transmits them to the reference sensor.
- Step 4: After receiving the pressure and temperature data from the last measurement sensor, the reference sensor sends a Finish command, synchronously performs dynamic differential processing, and outputs the results to the cloud platform.
- Step 5: After receiving the Finish command, each measurement sensor enters a sleep state and waits for the next measurement to begin.

According to the above ideas, in this study, we designed and packaged the hardware structure of the reference and measurement sensors on the basis of embedded and IoT transmission technologies.

For a reference sensor, the functions that should be completed are shown below.

- (1) Real-time collection of air pressure and temperature data as reference pressure and temperature, respectively
- (2) Communicating with each measurement sensor to obtain real-time measurement data
- (3) Real-time dynamic differential processing of the data and outputting of the results to the cloud platform

Owing to the large amount of data that should be processed, we used STM32 series chips with strong performance as the main control chip to control the data exchange between the LoRa wireless communication module and the measurement sensor, controlled the barometer chip to obtain the pressure and temperature of the reference sensor, and controlled the 4G wireless

communication module to interact with the platform. The hardware structure diagram is shown in Fig. 1.

For measurement sensors, only the functions that should be completed are shown below.

- (1) Real-time collection of air pressure and temperature data at the location to be measured
- (2) Communication with the reference sensor to output real-time measurement data

Therefore, we used an Arduino microcontroller as the main control chip, controlled the barometer chip to obtain the pressure and temperature of the measurement sensor, and controlled the data exchange between the LoRa wireless communication module and the reference sensor. The hardware structure diagram is shown in Fig. 2.

The barometer chip used in this study is BME680, which is a four-in-one MEMS environment sensor that can measure volatile organic compounds, temperature, humidity, air pressure, and so forth. Owing to the use of MEMS technology,^(18,19) the sensor has a small size and low power consumption. The core parameters are as follows: the temperature measurement range is from -40 to $+85$ °C and the temperature measurement accuracy is ± 1.0 °C. The air pressure measurement range is from 300 to 1100 hPa and the air pressure measurement accuracy is ± 0.6 hPa.

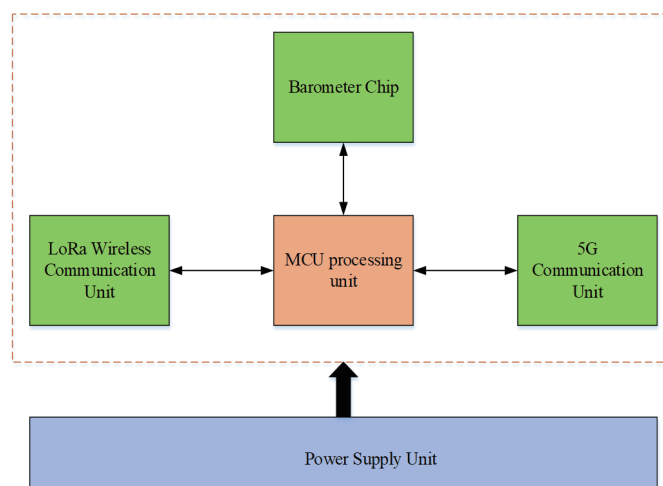


Fig. 1. (Color online) Hardware structure diagram of reference height sensor.

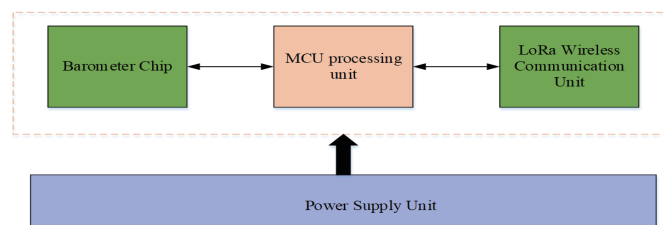


Fig. 2. (Color online) Hardware structure diagram of measurement sensor.

To facilitate experimental measurement, the sensors have been packaged in this study, and the physical image is shown in Fig. 3. Each sensor has a vent hole designed at the bottom to ensure consistency with the external atmosphere.

4. Test and Results

We built a real-time dynamic differential measurement system on the basis of the above measurement principles and prepared sensors. The system includes one measurement sensor and one benchmark sensor, and the final data is received by the cloud platform.

Before measurement, we first performed the zero-point calibration of the two sensors, and the initial states of the two sensors were measured as shown in Table 2.

The initial height measured in Table 2 is obtained on the basis of the standard international atmospheric pressure height formula. It is a height relative to sea level. It is necessary to perform a zero-point calibration based on the actual height of the sensor during on-site measurement to obtain the actual height of the measured object relative to the ground.

To compare and analyze the effects of dynamic differential measurement, we used the standard international atmospheric pressure height formula to calculate the elevation of the measurement sensor based on its pressure data after a zero-point calibration using the dynamic differential measurement method.

During the test, the measurement sensor was placed on the lifted object, and five height values were randomly selected, each of which remained for a period of time to facilitate the



Fig. 3. (Color online) Physical image of sensor.

Table 2
Initial states of sensors.

Category	Initial pressure (Pa)	Initial temperature (°C)	Actual initial height (m)	Measured initial height (m)
Reference sensor	100145	38.69	0.33	98.58
Measurement sensor	100148.6	38.52	0.33	98.35

recording of relevant data. At each elevation, a laser ranging method was used to measure the actual height of the measurement sensor from the ground. The elevation settings are shown in Table 3.

With the standard international atmospheric pressure height formula, the elevation of the measurement sensor can be obtained as shown in Fig. 4.

Figure 4 shows that the actual measured elevation coincides with the design elevation, but at each elevation, there are significant fluctuations in measurement results, which are caused by atmospheric pressure fluctuations. According to Eq. (9), when the atmospheric pressure fluctuates by 1 Pa, the elevation changes by about 8 cm. During the actual measurement, since the position of the reference sensor does not change, the pressure fluctuation of the reference sensor can be observed to reflect the pressure fluctuation in the measurement area, as shown in Fig. 5. It can be seen from the figure that the pressure fluctuation range can reach 10 Pa during the actual measurement.

Table 3
Elevation settings.

Order number	0	1	2	3	4	5
Elevation (m)	0.33	1.03	1.61	2.49	3.19	5.45

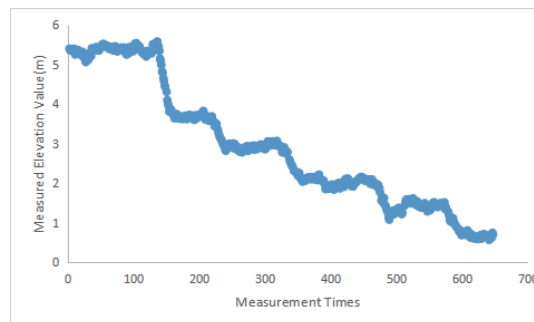


Fig. 4. (Color online) Measurement results obtained when directly using the standard international atmospheric pressure height formula.

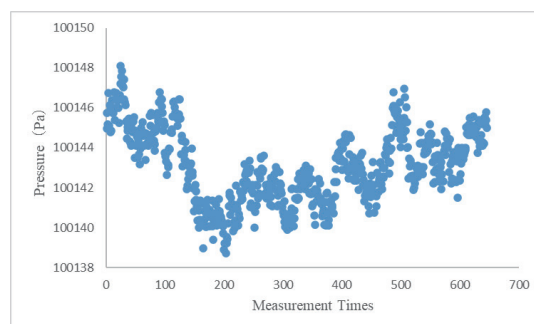


Fig. 5. (Color online) Pressure fluctuation of reference sensor.

Therefore, in actual measurement, it is necessary to use differential measurement methods to eliminate the elevation error caused by atmospheric pressure fluctuations. Figure 6 shows the dynamic differential measurement results obtained by the cloud platform. From the results, all set heights are distinctly measured using dynamic differential measurement methods, and the measured elevations are consistent with the set elevation, indicating that the dynamic differential measurement system in this study can be used to accurately and stably measure elevation.

Taking the average measurement value of each elevation as the elevation measurement result, we determined the error between the actual measurement result and the design elevation as shown in Table 4. The results show that the maximum measurement error after the dynamic differential measurement is reduced from 39 to 4 cm, effectively improving the measurement accuracy, which is higher than the accuracy of 5 cm achieved by GNSS technology in Ref. 6 and the accuracy of 84 cm achieved using a barometer in Ref. 12.

In addition, Fig. 6 shows that the measured elevation values at each height fluctuate around a certain distance, indicating that there is a certain error in the measurement. This is due to the fact that the pressure fluctuations of the reference and measurement sensors are not exactly the same, and there may be random fluctuations in pressure near the measurement point. At the same time, the measurement accuracy of the sensor itself can also lead to errors in the measured values. To reduce such errors, the average filtering method is generally used for data processing. Traditional arithmetic average filtering requires multiple samples to obtain a valid value. Although it can improve accuracy, it manifests as a slow response of the system. Therefore, we

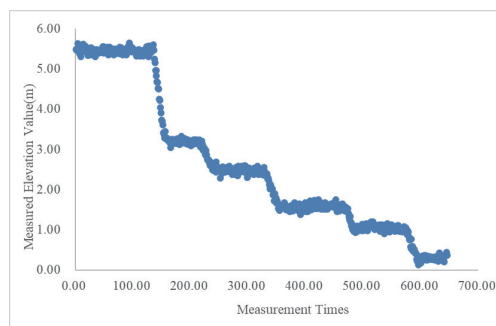


Fig. 6. (Color online) Real-time dynamic differential measurement results.

Table 4

Results of elevation obtained by dynamic differential and direct measurements.

Elevation designed (m)	Dynamic differential measurement		Direct measurement	
	Measurement value (m)	Measurement error (m)	Measurement value (m)	Measurement error (m)
1.03	1.02	0.01	1.41	0.38
1.61	1.65	0.04	2.00	0.39
2.49	2.53	0.04	2.78	0.29
3.19	3.2	0.01	3.57	0.28
5.45	5.49	0.04	5.37	0.08

selected the sliding average method for the real-time processing of atmospheric pressure data. This method averages the current sampling value with previous continuous historical sampling values, so that effective values can be obtained at the end of each sampling, which can considerably improve the system response rate.^(20,21) The core is the selection of the size of the sliding window. Excessive sliding window values may cause sensor response delays. Therefore, considering the timeliness of the measured data, we used a sliding window of 5 to perform arithmetic average filtering, that is, starting from the sixth sampling data, the system outputs the elevation. Figure 7 shows the measurement results obtained after moving average filtering. As can be seen from the figure, the fluctuation in elevation has significantly decreased.

Figure 7 also shows that after the noise is eliminated by the moving average method, the measurement results are clearly stable. At the same time, compared with the results obtained before the noise removal, it can be seen that the real-time performance of the data is not affected, which shows that the moving average method used in this study is effective. We performed data denoising without reducing the real-time measurement performance.

Figure 8 shows that before using the moving average method to denoise, the error fluctuation range is ± 15 cm, and after using the moving average method to remove noise, the error fluctuation range is ± 5 cm. Therefore, the combination of real-time dynamic difference and moving average denoising can effectively improve the measurement accuracy of the barometer elevation, making it practical for engineering.

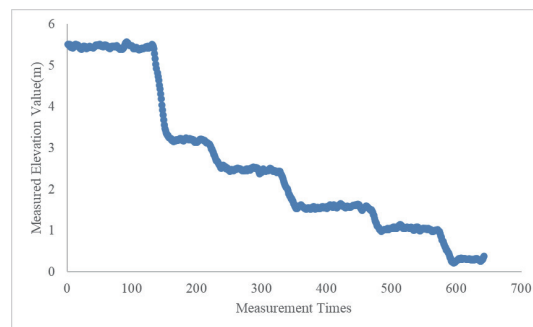


Fig. 7. (Color online) Moving average measurement results.

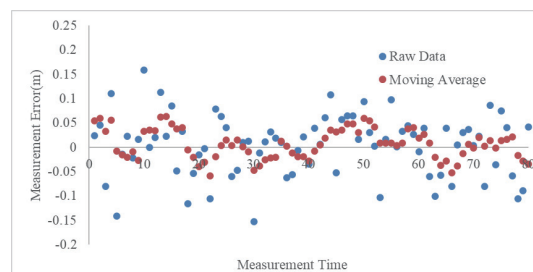


Fig. 8. (Color online) Comparison of measurement results obtained before and after moving average filtering.

5. Conclusions

First, we expounded on the relationships among elevation, pressure, and temperature from the isothermal atmospheric pressure model and the international standard atmospheric pressure height formula theory. On the basis of the idea of differential measurement, a mathematical model for the dynamic differential measurement of atmospheric pressure sensors was established. Then, on the basis of IoT and embedded technologies, a high-precision elevation sensor based on atmospheric pressure and dynamic difference was developed, and a reference height sensor and a measurement height sensor were designed and fabricated. The working principle of the dynamic differential measurement system was described. On this basis, a dynamic differential measurement experiment was conducted, and the results showed that the proposed dynamic differential height measurement scheme based on a barometer reduced the measurement error from 39 to 4 cm compared with the direct measurement method. To further optimize the real-time measurement accuracy, we proposed a moving-average-based elevation data processing method. The real-time measurement error was reduced from ± 15 to ± 5 cm, whereas the measurement frequency remained unchanged, and the high-precision elevation sensor has good engineering practicality.

References

- 1 W. Zhao, J. Li, J. Zhao, T. Jiang, J. Zhu, D. Zhao, and J. Zhao: IET Microw. Antenna. **14** (2020) 1547. <https://doi.org/10.1049/iet-map.2019.1136>
- 2 N. Zhang, S. Yan, W. Wang, and J. Gong: Prog. Electromagn. Res. M **77** (2019) 73. <https://doi.org/10.2528/PIERM18101402>
- 3 Z. M. Wani and M. Nagai: Measurement **177** (2021) 109311. <https://doi.org/10.1016/j.measurement.2021.109311>
- 4 Y. Li, Z. Zhang, X. He, H. Yuan, and N. Zang: Meas. Sci. Technol. **34** (2023) 015011. <https://doi.org/10.1088/1361-6501/ac900d>
- 5 O. Roggenbuck, J. Reinking, and T. Lambertus: Remote Sens. **11** (2019) 1. <https://doi.org/10.3390/rs11040409>
- 6 J. Strandberg, T. Hobiger, and R. Haas: GPS Solutions **23** (2019) 1. <https://doi.org/10.1007/s10291-019-0851-1>
- 7 J. Strandberg, T. Hobiger, and R. Haas: IEEE Geosci. Remote Sens. Lett. **14** (2017) 1552. <https://doi.org/10.1109/LGRS.2017.2722041>
- 8 Y. Li, Z. Zhang, X. He, Y. Wen, and X. Cao: Measurement **197** (2022) 11342. <https://doi.org/10.1016/j.measurement.2022.111342>
- 9 X. Cao, X. Yu, Y. Ge, T. Liu, and F. Shen: Measurement **195** (2022) 111134. <https://doi.org/10.1016/j.measurement.2022.111134>
- 10 G. Ai, H. Shi, H. Wu, Z. Li, and J. Guo: Sci. China Ser. G-Phys. Mech. Astron. **52** (2009) 472. <https://doi.org/10.1007/s11433-009-0065-6>
- 11 G. Ai, P. Sheng, J. Du, Y. Zheng, X. Cai, H. Wu, Y. Hu, Y. Hua, and X. Li: Sci. China Ser. G-Phys. Mech. Astron. **52** (2009) 376. <https://doi.org/10.1007/s11433-009-0060-y>
- 12 H. Xia, X. Wang, Y. Qiao, J. Jian, and Y. Chang: Sensors **15** (2015) 1. <https://doi.org/10.3390/s150407857>
- 13 H. Choo, B. Lee, H. Kim, and B. Choi: Autom. Constr. **147** (2023) 104714. <https://doi.org/10.1016/j.autcon.2022.104714>
- 14 Y. Zhao, J. Liang, X. Sha, J. Yu, H. Duan, and G. Shi: IEEE Access **7** (2019) 84680. <https://doi.org/10.1109/ACCESS.2019.2924664>
- 15 D. E. Bolanakis: IEEE Instrum. Meas. Mag. **20** (2017) 30. <https://doi.org/10.1109/MIM.2017.8121949>
- 16 P. Liu, W. Zhang, T. Wang, X. Jia, Y. Ma, K. Jia, and Y. Wang: Intell. Autom. Soft Comput. **33** (2022) 855. <https://doi.org/10.32604/iasc.2022.022380>
- 17 M. Hou, Y. Wang, F. Zhu, Y. Wang, and C. Liao: 2017 25th Optical Fiber Sensors Conf. (OFS) (IEEE, 2017) 108532. <https://doi.org/10.1117/12.2262316>
- 18 H. Rene, M. Mierka, V. Jancarik, M. Bittera, J. Halgos, M. Dzuris, J. Krchnak, J. Hricko, and R. Andok: Sensors **23** (2023) 1. <https://doi.org/10.3390/s23031241>

- 19 X. Zhang, D. Qiao, and Y. Zhu: J. Micromech. Microeng. **33** (2023) 035006. <https://doi.org/10.1088/1361-6439/acba28>
- 20 Z. Pan, X. Wang, T. T. G. Hoang, and L. Tian: Int. J. Electr. Power Energy Syst. **149** (2023) 109021. <https://doi.org/10.1016/j.ijepes.2023.109021>
- 21 Z. Chang, Q. Gao, G. Monti, H. Yu, and S. Yuan: Soil Dyn. Earthquake Eng. **164** (2023) 107574. <https://doi.org/10.1016/j.soildyn.2022.107574>

About the Authors



Gou Jie received her B.S. and M.S. degrees from Chang'an University, China, in 2002 and 2005, respectively. From 2005 to 2010 and from 2011 to 2012, she was a lecturer and an assistant professor, respectively, at GuiZhou Communications Polytechnic, China. Since 2012, she has been an assistant professor at Wuhan Technical College of Communications. Her research interests are in road and bridge engineering technology. (20456150@qq.com)



Hao Zhu received his B.S. and M.S. degrees from ChangAn University, China, in 2002 and 2005, respectively. Since 2005, he has been a senior engineer at CCCC Second Harbor Engineering Company Ltd. His research interests are in bridge construction monitoring, health monitoring, and sensor development. (15527752@qq.com)



Huadong Yang received his B.S. and M.S. degrees from Wuhan University of Technology, China, in 2014 and 2018, respectively. From 2018 to 2021, he was an R&D engineer at Yangtze Optical Fibre and Cable Joint Stock Limited Company, China. Since 2021, he has been a deputy chief engineer of the Intelligent Construction Department at CCCC Second Harbor Engineering Company Ltd. His research interest is in sensors. (464179071@qq.com)